Solvation Behavior of Cellulose and Xylan in the MIM/EMIMAc Ionic Liquid Solvent System: Parameters for Small-Scale Solvation

Susanne Bylin,[a,c] Carina Olsson,[b] Gunnar Westman,[b,c] and Hans Theliander [a,c,*]

Ionic liquid treatment has been reported by several researchers as a possible step in the process of fractionating lignocellulosic biomass within the biorefinery concept. However, understanding how solvation can be achieved and how the feedstock biopolymers are affected is needed prior to a viable implementation. An effective two-component solvent system for the wood components cellulose and xylan has been developed. Furthermore, the solvation of these components in the system consisting of the ionic liquid (IL) 1-ethyl-3-methylimidazolium acetate (EMIMAc) in a novel combination with the co-solvent 1-methylimidazole (MIM) is investigated. Focused beam reflectance measurement (FBRM) particle characterization in combination with microscopic analysis and molecular weight determinations (xylan) shows that cellulose and xylan can be most efficiently solvated using only 3 to 4% IL (n/n anhydro-glucose units and n/n anhydro-xylose units) and 9% IL, respectively, while still avoiding any significant polymer degradation. A model for a two-step process of cellulose solvation in the present system is proposed.

Keywords: Ionic liquid; Solvation; Cellulose; Xylan; FBRM

*Contact information: a,b: Department of Chemical and Biological Engineering, Chalmers University of Technology, SE-412 96, Gothenburg, Sweden; a: Division of Forest Products and Chemical Engineering; b: Division of Chemistry and Biochemistry, Organic Chemistry; c: Wallenberg Wood Science Center, The Royal Institute of Technology and Chalmers University of Technology, SE-100 44, Stockholm, Sweden; * Corresponding author: hanst@chalmers.se*

INTRODUCTION

The Biorefinery

With the global advent of biorefineries, the need has emerged for the development of new processes and studies of their implications on the physical and chemical properties of biomass and its components. Biomass of all types (*e.g.*, bagasse, algae, and wheat) is being considered for this purpose, and depending on their origin and composition, the products from these biorefineries can be used for material, chemical, fuel, or energy purposes. Wood, as a globally widespread and renewable biomass resource, is highly suitable for the biorefinery concept. Because forests and agricultural crops grow in different soil types under normal circumstances, woody biomass also has the advantage of not competing with agricultural crops when it comes to land exploitation. However, the topic is under debate (Elnashaie *et al.* 2008; Rettenmaier *et al.* 2010).

The Borregaard Biorefinery in Sarpsborg, Norway, is one example of a currently operating biorefinery that utilizes wood as feedstock in its process. This biorefinery is a converted sulfite pulping mill that currently produces lignin, cellulose pulp of various

qualities, bio-ethanol, vanillin, and some smaller side streams (Rødsrud *et al.* 2012). Liu *et al.* recently published a review article on the subject of the woody biorefinery in which a seven-step process to "incrementally decompose" wood material is suggested: "1) hot-water extraction, 2) hydrolysis, 3) separation of xylan, sugars, and acetic acid, 4) fermentation, 5a) pulping of hot-water-extracted wood chips followed by pulping and paper-making, 5b) the use of extracted wood chips/woody biomass for reconstituted wood products such as particle board, and 5c) further separation/hydrolysis of the extracted woody biomass to platform chemicals: aromatics and wood sugars." To achieve such selective decomposition in a controlled manner, the separation and solvation behavior of each component needs to be studied in great detail. Liu's suggestion is based on current research in wood pre-treatments being conducted worldwide.

Many proposed methods of pre-treatment to date include mechanical, chemical, and enzymatic procedures (Brodeur *et al.* 2011; Liu *et al.* 2012b). One option for the chemical pre-treatment of wood or other lignocellulosic biomass is the solvation of fractions enriched with certain wood components by means of solvent extraction, for example, using ionic liquids (ILs).

Ionic Liquid Solvent Systems

Ionic liquids (ILs) are a class of liquids that were first discovered around the turn of the last century and had a strong renaissance in the early 2000s. The class is defined as any ionic compound with a melting point below 100 °C. These molten salts can for example be used as solvents. A more defined sub-class is room-temperature ionic liquids (RTILs), which are in a liquid state below room temperature (Laus *et al.* 2005; Linhardt 2005). Ionic liquids have been shown to dissolve materials that are otherwise difficult to dissolve, such as wood and other lignocellulosics, even when using milder conditions than the traditional method of cooking biomass (Fukaya *et al.* 2008; Muhammad *et al.* 2011).

The interest in ILs in the biomass processing field began in 2002, when the neat imidazolium salt 1-butyl-3-methyl imidazolium chloride (BMIMCl, Fig. 1a) was first found to dissolve cellulose (Swatloski *et al.* 2002).

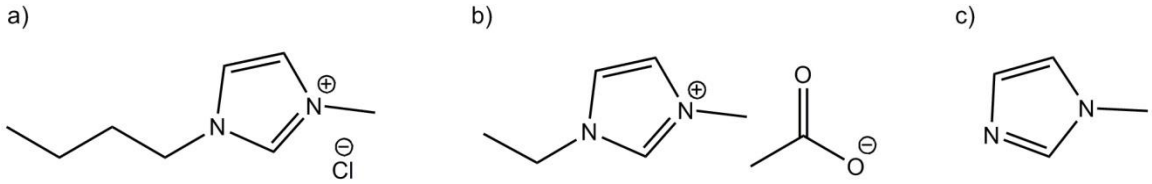

Fig. 1. Molecular structures of a) the first cellulose-dissolving IL, 1-butyl-3-methyl imidazolium chloride (BMIMCl); b) the solvent IL of the present study, 1-ethyl-3-methyl imidazolium acetate; and c) the co-solvent of the present study, 1-methylimidazole (MIM).

It is common knowledge that ILs, including a number of cations and many different anions, are able to dissolve cellulose as direct solvents. The unique solvation properties, in combination with a low vapor pressure, make their possible industrial application of great interest. The most popular cation for cellulose applications is the imidazolium cation, along with variations of its alkyl substituents. The effect of alkyl chain length on cellulose solvation ability was acknowledged as early as 2002 by Swatloski and has since been observed by several groups (Swatloski *et al.* 2002; Vitz *et*

al. 2009). The asymmetrical cation gives these ionic liquids favorable viscosities, an important feature for a solvent, particularly in polymer applications. The efficiency of the IL 1-ethyl-3-methyl imidazolium acetate (EMIMAc, Fig. 1b) as a cellulose solvent is high, and a cellulose pulp loading of up to 20 wt% can be easily dissolved (Kosan *et al.* 2008). Apart from excellent solvation efficiency, EMIMAc has the advantage of being an RTIL, which means it has a low vapor pressure, thermal stability, a relatively high boiling point, and low melting point (Wendler *et al.* 2012).

Co-solvents may be added to modify solution properties such as viscosity, loading capacity, and solvent polarity. Appropriate co-solvents can be found by measuring solvatochromic parameters (Gericke *et al.* 2011; Gericke *et al.* 2012; Rinaldi 2011). As an additive, 1-methylimidazole (MIM, Fig. 1c) has been studied in solutions of BMIMCl and cellulose and has been found to drastically reduce degree of polymerization (DP) loss in cotton pulp (Liu *et al.* 2011). The interaction between cellulose, MIM, and IL is discussed in this article, but more research needs to be done to understand the effect of the co-solvent in this case.

Wood Biopolymers

The two most abundant polysaccharides in hardwood are cellulose and xylan (shown in Fig. 2). Native cellulose has a high DP, which inevitably leads to a decrease in solubility caused by a decrease in the entropic gain in the solvation process; glucose, cellobiose, and any oligomer of cellulose up to a DP of about 10 are soluble in simple solvents. Furthermore, three hydroxyl groups *per* anhydroglucose unit (AGU) facilitate complex patterns of hydrogen bonds, both intra- and inter-molecular. To overcome these bonding interactions, solvents with high hydrogen bonding capacities are necessary. Water alone cannot dissolve cellulose, despite the fact that pair-wise hydrogen bond interactions involving water-water, carbohydrate-water, and carbohydrate-carbohydrate hydrogen bond pairings all are approximately 5 kcal/mol (Lindman *et al.* 2010). It is obvious that hydrogen bonding is not the only relevant factor, and other types of interaction should be taken into consideration. Hydrogen bonds keep the linear cellulose chains arranged in sheets. Stacking of these sheets into the three-dimensional crystal structures of the cellulose material involves hydrophobic, or so-called van der Waals, interactions (O'Sullivan 1997; Vanderhart and Atalla 1984). Recently, a few publications have brought this matter forth for discussion (Bergenstråhle *et al.* 2008; Biermann *et al.* 2001; Cho *et al.* 2011; Gross and Chu 2010; Lindman 2010; Lindman *et al.* 2010). Because cellulose has both hydrophilic and hydrophobic features, *i.e.*, equatorial hydroxyl groups and axial hydrogen atoms, a good solvent should contain both a hydrogen bonding moiety and a hydrophobic moiety.

Xylan has long been seen as a by-product of little importance within the agricultural and forestry sectors. Although difficult to refine, the high content of xylan in both annual plants and trees has attracted scientific interest due to its potential in a variety of applications. It has already been shown that xylan can contribute to a range of properties in certain biomaterials, *e.g.*, in flexible transparent films with interesting gas barrier properties (Gröndahl *et al.* 2004) and as a component in aerogels for constructing porous nanofibers (Aaltonen and Jauhiainen 2009). As briefly mentioned, the biorefinery concept allows xylan to be isolated and either used without further modifications or hydrolyzed into xylose monomers for other uses. The diversity in substitution of extracted materials, both in terms of side group composition and the substitution pattern

of the xylan polymer backbone (Fig. 2b), depends largely on the plant origin, as well as on the extraction method (Fengel 2011).

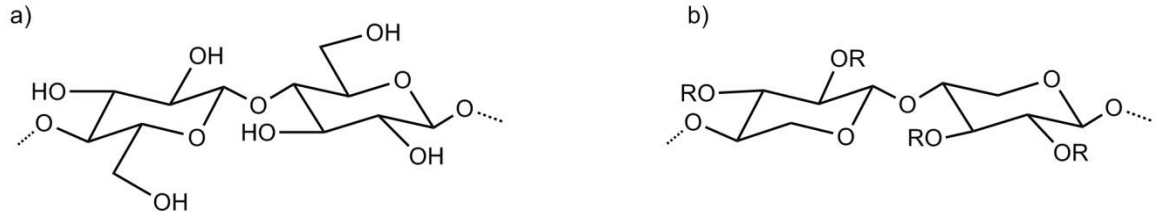

Fig. 2. Chemical structures of a) cellulose and b) xylan. For xylan, R is either a hydrogen or a substituent; acetyl and 4-O-methylglucuronic acid (MeGlcA) are found in hardwood xylans, while arabinofuranose is common in xylans from annual plants.

Xylan is a pentose and therefore lacks the C6 and its hydroxyl group, which has a large influence on cellulose solubility. On average, seven out of ten C3 positions in xylan are acetylated in hardwoods. Furthermore, every tenth or so C2 position carries the 4-O-methyl glucuronic acid (MeGlcA) side group (Aspinall *et al.* 1954). Softwoods have a somewhat different ratio of substitution and often include substitution of arabinofuranose in different ratios. This diversity makes the solubility of the xylan polymer hard to predict and highly dependent on factors such as pH and the ionic strength of the solvating system. At the same time, the substitutions in these positions mean that xylan does not pack into crystal structures in the way cellulose does, and the MeGlcA renders the polymer quite resistant to alkaline degradation, also called peeling reactions (Wigell *et al.* 2007). The DP for xylans varies between 100 and 200, as opposed to native cellulose, which has a DP of approximately 10,000 (Gírio *et al.* 2010; O'Sullivan 1997). The lower DP makes the positive entropy of mixing easier to overcome by, for example, heating the xylan sample mixtures.

To successfully implement an IL processing step in a future biorefinery a number of criteria need to be met; *e.g.* the cost and simplicity of attaining the ILs, minimizing the energy demand of the process, and providing high material efficiency. The choice of MIM as a co-solvent meets the first of these requirements since it is a pre-cursor in the industrial synthesis of EMIMAc itself, but it also satisfies the latter two. The current study is aimed at the improved understanding of the parameters that govern the solvation of the biomass components cellulose and xylan using this new combination of ionic liquid and co-solvent, with the goal of industrial application. Recovered and regenerated materials are analyzed in combination with *in situ* particle monitoring of the process.

Furthermore, the present "parameters for small scale solvation" study highlights solvation behavior on a small (20-mL glass vial) scale, with a focus on discussing the mechanisms of solvation in the new solvent system. The effect of fiber length is examined for the cellulose, and the effects of temperature and solvent concentrations for both cellulose and xylan. An ongoing experimental study focuses on solvation on a larger (250-mL glass reactor) scale under selected process conditions and the effect of these conditions on certain properties of the polymer components.

EXPERIMENTAL

Materials

Cellulose was obtained as a dissolving pulp from Borregaard AS in Sarpsborg, Norway. The pulp was pre-treated mechanically by Wiley milling and passed through a 1-mm sieve to ensure adequate and equivalent milling for all samples. Some material was passed through smaller sieves, giving three cellulose fractions: un-fractionated (< 1 mm), a large fiber fraction (0.5 mm < d < 1 mm), and a small fiber fraction (d < 0.088 mm). Sieve dimensions were chosen to provide one fraction representative of a fines population (d < 0.088 mm), and one for a population of longer fibers (0.5 mm < d < 1 mm). The dry content of the pulp was determined to be 97%. Beech xylan was purchased from Sigma Aldrich and was used without further processing. Characterization of the xylan showed a relative sugar composition of 94% xylose, 2.1% galactose, 2.1% glucose, 0.9% rhamnose, 0.6% arabinose, and < 0.1% mannose. Klason lignin and acid-soluble lignin (ASL) were determined to be 5.4% and < 1.0%, respectively. The ash content was found to be 4.9%. The ionic liquid 1-ethyl-3-methylimidazolium acetate (≥ 90% purity) and the co-solvent 1-methylimidazole (≥ 99% purity) were obtained commercially from BASF and Sigma-Aldrich, respectively. Both solvents were kept under inert atmospheres and were used without further processing.

Methods

Solvation experiments

The solvation of both un-fractionated and fractionated cellulose fibers and xylan was studied for a 3.5 wt% polymer solution on a small scale. The study was performed at 50 °C for un-fractionated and fractionated materials, at 30 °C for the fractionated material, and at 50 °C and 70 °C for xylan. Temperatures were chosen to represent one lower, yet easily controlled temperature (30 °C) and one higher, yet still considered low for industrial application (50 °C), for cellulose. Preliminary testing showed that xylan was not soluble at 30 °C; hence the two temperatures chosen for solvation of xylan represents one lower for comparison to cellulose solubility (50 °C), and one higher for assessment of potential polymer degradation (70 °C). The molar ratio of IL to monomer (anhydro-glucose unit, AGU, and anhydro-xylose unit, AXU) ranged from 0 to 4 (samples C0-C4 (Table 1) for cellulose, and from 0 to 21 (samples X0-X21, Table 2) for xylan.

Table 1. Total Content of IL in Cellulose Samples C0-C4 Compared to the Combined IL and MIM Content in Each Sample

Sample ID (mol IL/mol AGU)	%IL (n/n)	%IL (w/w)	%IL (V/V)
C0	0	0	0
C1	2	4	3
C2	4	8	5
C3	6	11	8
C4	8	15	11

Number notations in sample names C0-C4 refer to molar amount of IL per AGU.

Solvation upon IL batch addition was studied using optical microscopy and focused beam reflectance measurements (FBRM, see *Physical characterization* section) after 4 h of stirring at a set temperature, and samples were re-checked after 24 h. Samples were pre-dispersed in MIM (30 min) in 20-mL screw-cap glass vials prior to IL addition. Temperature and rpm were controlled throughout the experiments. After solvation, xylan samples were filtered through a glass filter (Whatman, RGB, 90 mm) using vacuum filtration, which resulted in residual fractions X0(1)-X21(1). The xylan was thereafter regenerated in warm EtOH (50 °C). Subsequent filtration resulted in regenerated fractions X0(2)-X21(2). All xylan fractions were characterized using Klason lignin and ASL protocols found in the literature (Dence 1992; Theander and Westerlund 1986). High-performance liquid chromatography (HPLC) and gel-permeation chromatography (GPC) were performed to determine the relative sugar compositions and molecular weight distributions using methods and instruments described in the chemical characterization section.

Table 2. Total Content of IL in Xylan Samples X0-X21 Compared to the Combined IL and MIM Content in Each Sample

Sample ID (mol IL/mol AXU)	%IL (n/n)	%IL (w/w)	%IL (V/V)
X0	0	0	0
X3	7	14	10
X6	16	29	21
X9	26	43	33
X12	38	57	46
X15	53	70	61
X18	71	84	78
X21	100	100	100

Number notations in sample names X0-X21 refer to molar amount of IL per AXU.

Physical characterization

For the analysis and characterization of the undissolved particles in the samples, an *in situ* FBRM G400 probe with a laser scanning speed of 2 m/s was used (Mettler-Toledo AutoChem Inc.). The probe was used with the iC FBRM software version 4.2.234 SP1. The FBRM tool has been used previously to monitor real time changes to particle dimensions in dispersions, verifying phenomena such as flocculation, crystallization, and dissolution. Moreover, it is widely used in the pharmaceutical and paper-making industries (Coutant *et al.* 2010; Liu *et al.* 2013; Zakrajšek *et al.* 2009). The technique measures dynamic changes to an optical chord length distribution (CLD) of solid-liquid dispersions. The optical chord length is defined as a straight line between any two points in a particle dispersion perceived by the FBRM-laser as a particle edge. The FBRM signal is collected over 1324 primary channels over the size range of 1 to 1000 µm. The measurements were performed using the "fine" instrument setting, providing greater resolution for the first 400 channels (range: 0 to 100 µm with 0.25 µm channel widths). The back-scattered laser signal was displayed using logarithmic channel progression regrouping the chords over 90 channels and further visualizing these graphically as a chord length distribution. One should note that qualitative changes occurring to such a distribution during a measurement are not linearly correlated to the concentration of the

particles being measured. For instance, a chord of a larger particle is measured more often than that of a smaller one. This is important to keep in mind when analyzing FBRM data sets. In these experiments, data were collected every 2 s for 15 min, and a 10-sample moving average was then used to represent each sample. The measuring and data-handling principles and techniques are described in full elsewhere (Alfano *et al.* 1998; Coutant *et al.* 2010). All measurements were performed during a constant stirring of 250 rpm.

Further physical particle characterization was performed using optical light microscopy with a Carl Zeiss Discovery V12 SteREO microscope equipped with a KL1500 LCD cold light source. Images were recorded using AxioVision Software AxioVS40 V 4.7.2.0, Version 5.1.2600, Build 2600, SP3.

Chemical characterization

According to the literature protocol for Klason lignin determination (Theander and Westerlund 1986), milled (if particle d > 0.5 mm), pre-dried, and weighed samples (d < 0.5 mm, 105 °C, 12 h, 200 mg) were added to glass beakers (150 mL). Concentrated sulfuric acid (72% w/w, 3 mL) was then added; after careful stirring, the samples were allowed to impregnate under vacuum for 15 min. Beakers were transferred to a heat-regulated water bath (30 °C), where they were stirred every 20 min for a period of 1 h. For complete hydrolysis of the sugar polymers, the samples were then autoclaved at 125 °C for 1 h. Thereafter, samples were diluted with de-ionized water (84 g), and un-hydrolyzed material was filtered off as Klason lignin on a pre-weighed glass filter (Whatman, GF/A, 24 mm). After reaching room temperature (*ca*. 30 min), the filtrates were diluted in volumetric flasks (100 mL). A portion of the samples (5 mL) was further transferred to a new volumetric flask (50 mL), and a fucose standard (2 mL, 200 mg/L) was added to each sample before it was diluted up to 50 mL, and a final fucose concentration of 8 mg/L. Samples were further analyzed directly for ASL and filtered using a hydrophilic syringe filter (Acrodisc LC, d=13 mm, 0.45-µm PVDF membrane) before the relative sugar composition was determined.

ASL was determined using UV absorbance measurements with an absorptivity coefficient according to a protocol by Dence (Dence 1992). Measurements were performed in triplicate on a Specord 205 (Analytic Jena) at 205 nm.

Relative sugar composition was determined by chromatographic separation using high-performance anion exchange chromatography with pulse amperometric detection (HPAEC-PAD) and a gold reference electrode. The analysis was performed on a Dionex ISC5000 instrument with a Dionex AS-AP autosampler, using Dionex CarboPac PA1 columns (guard column 2 x 50 mm, pre-column 2 x 50 mm, and separation column 2 x 250 mm) and an AgCl reference electrode for pH calibration. A four-step instrument method was used, as follows: 1) column equilibration (10 min, 60% [200mM NaOH]; 40% [200mM NaOH, 170mM NaOAc]); 2) transition to H_2O (2 min, 100%); 3) sample injection; and 4) sample separation (25 min, 100% H_2O). The flow was constant at 0.260 mL/min. Data analysis was performed using Chromeleon 7 Chromatography Data System software, version 7.1.0.898.

Polymer degradation was assessed using molecular weight determinations by gel permeation chromatography (GPC). Analyses were performed using a PL-GPC 50 Plus integrated instrument system coupled with RI and UV detectors and equipped with a PL-AS RT auto-sampler for injections (Polymer Laboratories, Varian Inc.). Chromatographic separations were achieved using two PolarGel-M columns and a guard column (300 x 7.5

mm, 50 x 7.5 mm). Samples were pre-dissolved in the mobile phase (DMSO/LiBr, 10mM) and filtered through a syringe filter (GHP Acrodisc, d=13 mm, 0.2-µm GHP membrane) prior to analysis. Isocratic separation was performed with a flow rate of 0.5 mL/min. Data analysis was performed using Cirrus GPC software version 3.2. A 10-point calibration curve with Pullulan standards was used to determine molecular weights and DPs (708, 375, 200, 107, 47.1, 21.1, 11.1, 5.9, 0.667, and 0.180 kDa, Polysaccharide Calibrations Kit, PL2090-0100, Varian).

RESULTS AND DISCUSSION

Cellulose Solvation Experiments

Solvation of cellulose visually appeared to be complete within seconds. However, the first analyses were not performed until after 4 h to ensure no further solvation would occur. Figure 3 shows the fractionated materials after 4 h of dissolution for samples C0 through C4. Initially, no clear difference in solvation state regarding fiber length could be detected; however, when held up against the light, sample C2 with the longer fiber fraction was slightly less transparent than the C2 sample with the shorter fiber length. Entanglement of the fibers in the zero samples was also noted, as sedimentation of the long fiber fraction did not occur to the same degree as it did with the short fiber fraction.

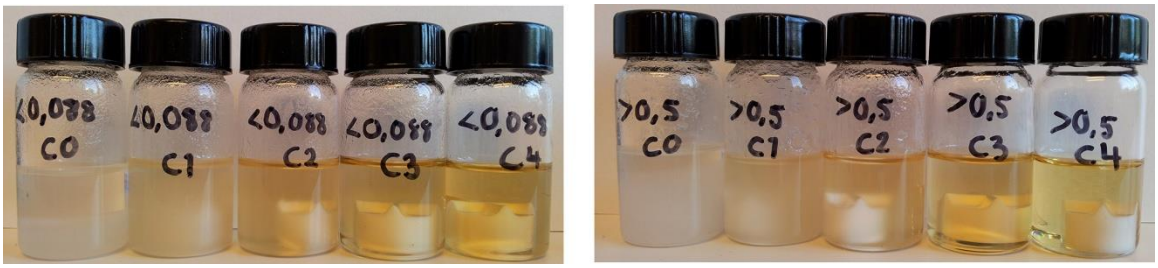

Fig. 3. Samples C0-C4 after 4 h of dissolution for the small fiber fraction (d < 0.088 mm) on the left and the large fiber fraction (0.5 mm < d < 1 mm) on the right (magnetic stir bars are visible in the clearer samples)

For all fractions, the greatest change in chord length distribution was found between samples C1 and C2 (Table 1), indicating that most of the cellulose fibers were solvated at this increase in IL concentration (Fig. 4b-f). This finding was also substantiated by the much higher apparent viscosity of sample C2 compared to that of C1 and C0, which is characteristic of polymer solutions. Furthermore, when applying a square-weighting filter to the FBRM data, a distribution maximum at *ca.* 25 to 30 µm—equivalent to that of a single fiber width—became apparent, making it possible to enhance the changes that occurred specifically related to this population (Fig. 4a). However, to avoid missing any potentially important data, the data set was analyzed without the use of weighting filters.

A difference in number of chords could be detected for the large *versus* the small fractions in the C1 samples. In these samples, the larger fraction is less dissolved at both temperatures studied (samples C1, Fig. 4c-f). This indicates a slight dependence of the amount of dissolved material on fiber length and that this dependence increases at the higher of the two temperatures.

Computer simulations have revealed that imidazole has a tendency to interact with glucose, primarily by means of hydrophobic stacking in an aqueous solution, and primarily on the H1-H3-H5-side of the glucose ring. In addition to hydrophobic stacking, the imidazole molecule might also act as a hydrogen bond acceptor (Chen *et al.* 2012; Youngs *et al.* 2007). Moreover, 1-methylimidazole is expected to exhibit analogous cellulose interactions. In addition, imidazolium-based cations have been found to interact with cellulose in a similar way. The imidazolium cation ring shows a weak affinity to the saccharide ring when cellulose is in the microfibril, but not in the solvated state. This can be explained by the presence of the many, much stronger interactions of the chloride counter ion with cellulose hydroxyl groups in the solvated state. Such interactions would effectively screen the cellulose, similarly to a hydration shell, and thereby block the much weaker interactions between the glucose ring and the imidazolium ring (Cho *et al.* 2011).

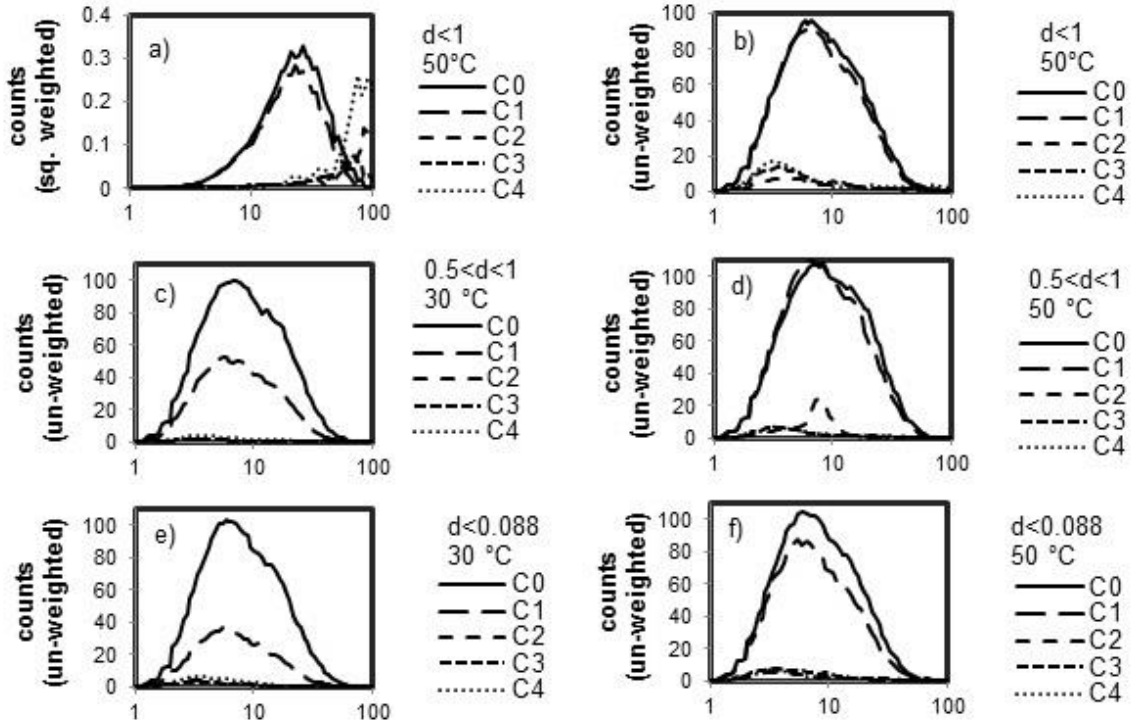

Fig. 4. Graphs a) and b) display square-weighted and un-weighted chord length distributions of un-fractionated cellulose fibers for IL concentrations C0-C4, respectively (molar amount of IL per AGU, see Table 1). Graphs c-f display un-weighted FBRM data for fractions 1 and 2 (e,f and c,d, respectively) at 30 °C and at 50 °C (c,e and d,f, respectively) for samples C0-C4. The small distribution seen in d) at about 9 µm is an artifact caused by a particle stuck on the probe window. All horizontal axes are in µm, and diameters [d] are in mm.

Because the molecular structure of MIM (Fig. 1c) is similar to that of the imidazolium cation and also to imidazole, it is therefore likely that these moieties interact with the cellulose structure in similar ways. This notion is further substantiated by other research groups, who have also demonstrated that the cation most likely interacts with the cellulose through hydrophobic interactions in spite of its ionic character (Liu *et al.* 2012a; Remsing *et al.* 2010). Because MIM by itself does not dissolve cellulose, the acetate anion is likely involved in overcoming the energy barrier for solubilization of the cellulose polymer. Liu *et al.* have shown that the anion stabilizes the cellulose gauche-

trans (gt) conformation of the C6-hydroxyl of cellulose II, as opposed to the trans-gauche (tg) found primarily in cellulose Iβ, or the gauche-gauche (gg) found primarily in cellulose III. They and others have further shown that the cation could in fact diffuse even into cellulose crystalline regions (Liu *et al.* 2012a; Rabideau *et al.* 2013).

Our study shows that in the present solvent system, three to four acetate ions are required per AGU for complete solvation. This is slightly more than one acetate ion per hydroxyl group present in the cellulose, indicating that all C6 hydroxyls likely need to be in a gt conformation to achieve solvation. This is in strong agreement with NMR-studies that have shown glucose hydroxyl-anion hydrogen bonding ratios of 1:1 and molecular dynamics simulations showing a predominant ratio being 4:5 (Youngs *et al.* 2007). In combination with the fast solvation of cellulose when EMIMAc is added, it is clear that the anions have little hindrance in reaching all free cellulose hydroxyls, even those further inside the microfibrils.

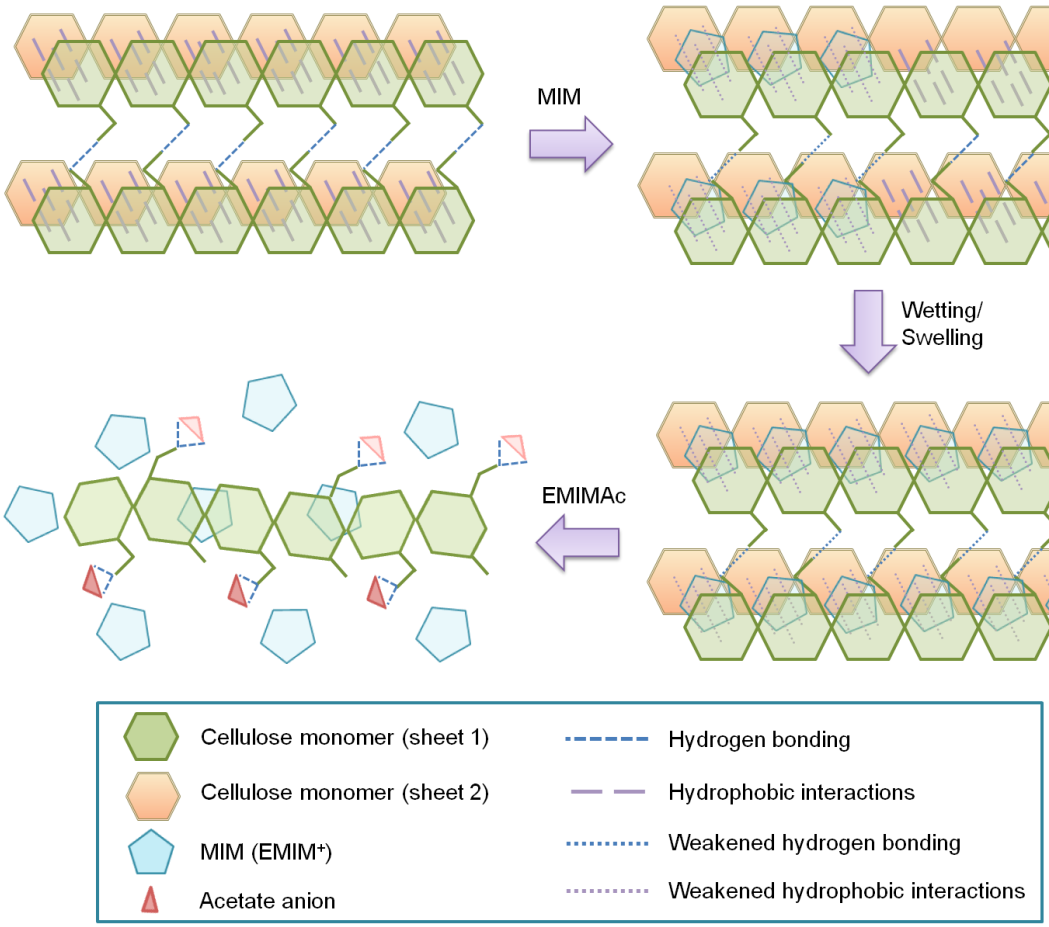

Fig. 5. Schematic representation of a possible route to solvation of cellulose in MIM/EMIMAc: Cellulose inter-sheet bonding is weakened as MIM solvent molecules form hydrophobic interactions with the cellulose chains. This would simultaneously weaken C6-OH – C3-OH hydrogen bonds, thereby giving the C6-OH a higher degree of rotational freedom. When EMIMAc is added, the gauche-trans conformation is stabilized throughout the chain. This gives rise to conformational changes that solvate the cellulose chains. The relatively strong cellulose-acetate interactions proceed to keep the cellulose chains solvated, even with continued addition of co-solvent. For clarity, only inter-chain C6-OH – C2-OH and C6-OH – OAc moieties and hydrogen bonds are depicted.

It is plausible that the extra acetate ions are required to stabilize the solvated state of the chains by means of hydrogen bonding interactions to C2- and C3-hydroxyls. These anion interactions would be comparable to the chloride ion interactions mentioned earlier (Cho *et al.* 2011). A schematic illustration for a proposed route to solvation (based on the above discussions) is presented in Fig. 5. An initial pre-"swelling/wetting" of the cellulose takes places in MIM, where the van der Waals forces between the cellulose sheets are first weakened. The importance of overcoming these inter-sheet hydrophobic interactions to efficiently dissolve cellulose has recently been stressed by several researchers (Gross and Chu 2010; Lindman *et al.* 2010).

A weaker cellulose sheet-packing would add rotational freedom to the C6 hydroxyl group that is involved in intermolecular bonding to the C3 hydroxyl group of the neighboring chain in cellulose I. Moreover, the C6 hydroxyl is less sterically hindered than the C2 and C3 hydroxyls, even though these are in equatorial positions. Therefore, it most likely interacts more strongly with the bulkier acetate anion than with, for example, the previously mentioned chloride anion. Once the energy barrier to the gt conformation is lowered, the acetate ion is assumed to stabilize the C6 hydroxyl in this position along the polymer chain, thereby facilitating the conformational changes required for solvation to proceed. This process would be further aided by the aforementioned extra acetate-hydroxyl interactions and a gain in entropy as the many non-specific MIM-cellulose interactions are lost when the acetate ions are introduced to the mix. The relatively strong bond of the acetate anion to the hydroxyl groups of 14 kcal/mol (Liu *et al.* 2010) is assumed to keep the anion associated to the cellulose chain, even if additional co-solvent is later added, thus keeping the cellulose in solution.

Solvation in the present system proceeds through a ballooning mechanism observed from 2 mol % of IL per AGU (Fig. 6, column C2). The phenomenon has previously been reported to occur during solvation in cold alkali (NaOH), NMMO (Lyocell process), and IL/DMSO systems (Cuissinat *et al.* 2008). The exact origin of the ballooning effect is not yet fully understood.

The micrographs in Fig. 6 further substantiate the significant change in fiber properties between samples C1 and C2 recorded by the FBRM. Moreover, upon the addition of small amounts of IL (C1), the fibers were less solvated at the higher temperature (Fig. 4c-f). This result was only detectable with the use of the *in situ* FBRM probe. To make similar detections by microscopic means, a huge data set would have to be sampled and analyzed, and image analysis software would likely be needed. The temperature effect was noticeable in both fractions, but was more pronounced in the long fiber fraction (Fig. 4c,d). Most likely this is an entropic effect and is probably caused by cellulose aggregation. It is believed that cellulose can adopt conformations that create surfaces of different hydrophobicities at different temperatures (Medronho *et al.* 2012). Therefore, cellulose would decrease or increase the net strength of the inter-sheet hydrophobic interactions depending on the temperature in the chemical surrounding.

Generally, as temperature increases, so does the internal energy of the polymer. This would weaken any bonding interactions of the cellulose, a phenomenon that counteracts the mentioned entropic effect on the route toward solvation. In the current solvent system, entropic effects thus dominate the solvation behavior under set conditions.

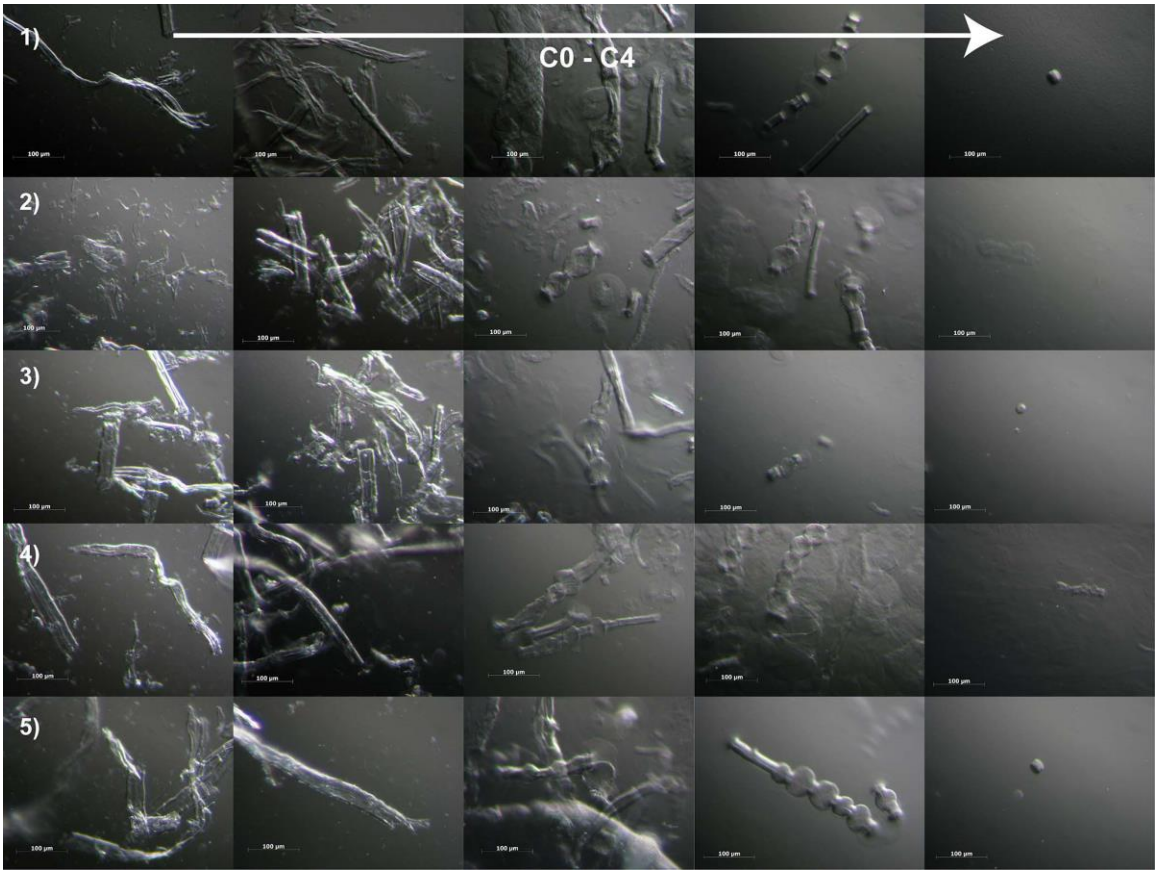

Fig. 6. Micrographs show solvation in samples C1-C4 (from left to right) for material that is 1) un-fractionated at 50 °C, 2) fractionated with d < 0.088 mm at 30 °C, 3) fractionated with d < 0.088 mm at 50 °C, 4) fractionated with 0.5 < d < 1 mm at 30 °C, and 5) fractionated with 0.5 < d < 1 mm at 50 °C, according to row numbering. The width of one micrograph is roughly 460 µm.

Xylan Solvation Experiments

Xylan solvation was observed to be slower than cellulose solvation. However, xylan samples appeared to be solvated after 4 h. In early attempts, ordinary stir bars were used during the solvation, but these proved inadequate for keeping the xylan particles sufficiently dispersed during the process. This led to large, sticky aggregates clumping together at the bottom of the vial. The problem was solved using cross-shaped stir bars that allowed for less sedimentation, even with dense particles. This problem highlights the importance of mixing and thus providing sufficient solvent/solute interaction interfaces during solvation. This is particularly true for working with polymers, where solvation is often slow. In contrast to all other samples, X9 was found to give the best solvation both at 50 °C and 70 °C, indicating an optimum solvation media at 26% ionic (n/n) (Fig. 7) and 9 moles of IL per AXU.

As mentioned in the introduction, the diversity of xylans makes the solubility of the polymer difficult to predict, and factors of importance are the substitution pattern and DP of the xylan, as well as pH and ionic strength of the solvating media. An optimum of these factors is evidently found in the X9 sample treatment for the xylan used. Solubility increased vastly upon raising the temperature without causing any significant degradation. Almost all molecular weight values fell within the standard deviation (1.5 kDa) of the reference xylan. The only samples that diverged from this behavior were

found in the regenerated samples X6(2) at both temperatures, which fell just below the standard deviation limit. The undissolved sample, X6(1), treated at 50 °C, showed a lower amount of xylan than the other samples. These results could indicate a slight degradation in the X6 sample treatment. However, further experiments need to be performed to establish this.

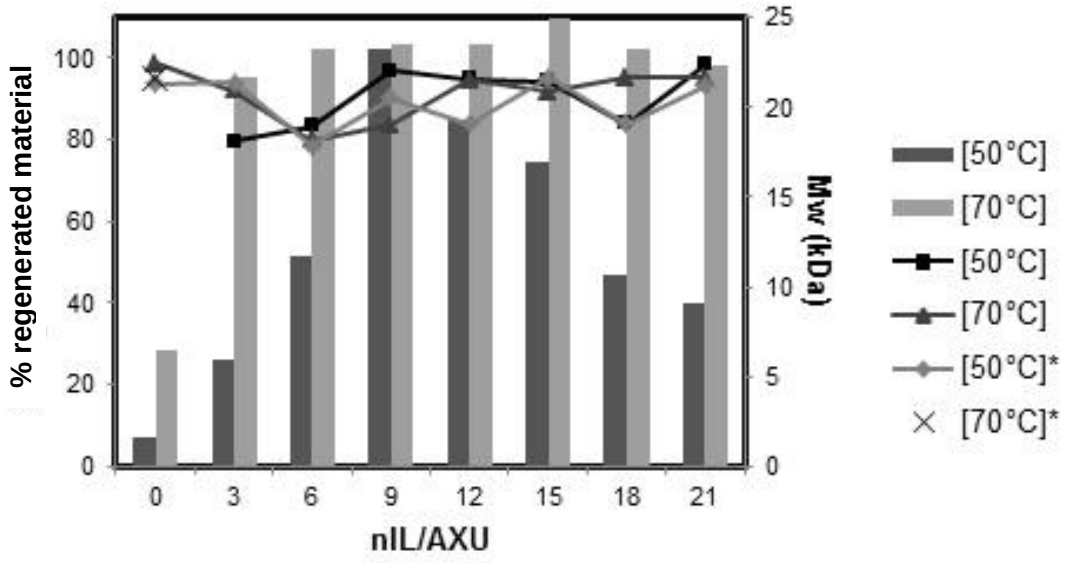

Fig. 7. The bars display the amount of regenerated material after xylan solvation at 50 °C and at 70 °C for samples X0-X21 (Table 1). Line plots display *Mw* for residual* and regenerated materials of the same. Untreated xylan had an *Mw* of *ca*. 21 kDa (standard deviation of 1.5 kDa).

The high dependence of xylan solvation on temperature is as expected because the lower DP and lack of crystal packing of xylans as compared to cellulose mean that the entropic resistance to solvation is much smaller. Furthermore, because MIM is a relatively hydrophobic liquid, solubility of the xylan should initially increase as the concentration of the highly polar organic molten salt (IL) is increased. This is precisely what is observed in the data set for the 50 °C samples (dark bar diagram in Fig. 7). After a concentration of 9 mol % IL in the sample is reached, the solubility is again reduced upon further addition of IL.

It should be noted that the apparent viscosities of the samples also increase as the more viscous IL is added, and this likely affects the solubility to some extent because solvent/solute transport becomes more hindered. However, when samples were rechecked after 24 h (prior to regeneration), no clear changes in solvation state were detected.

Xylan was furthermore observed to form aggregates under certain conditions (Fig. 8a, X12-X21). The aggregates were formed at higher concentrations of ionic liquid (*i.e.*, higher ionic strength) and could thus be partly attributed to the polymer "salting-out" of the solution.

Salting-out can be expected to be less pronounced at higher temperatures, where solvent capacity is higher, and thus the involvement of a salting out mechanism agrees with the data presented. Consequently, and because degradation in all the xylan samples was low, solvation is largely attributed to the chemical and physical behavior of the polymer in the solvent system. Because solubility was controlled by varying the MIM-to-EMIMAc ratio, it is plausible that similar solvation optima can also be established for

other xylans, for example, those isolated from biorefinery feedstock at different points in the process.

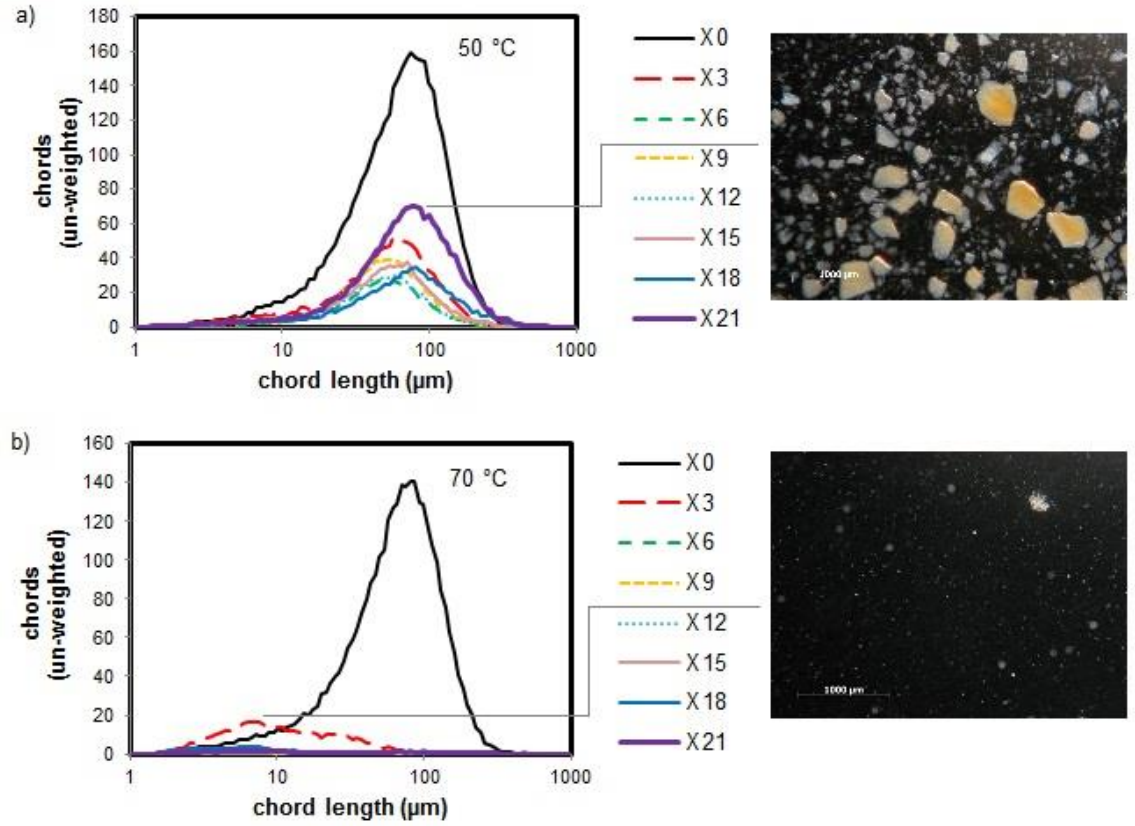

Fig. 8. FBRM data from both temperature series are displayed in graph a) for 50 °C and in b) for 70 °C. The micrograph in a) shows xylan aggregation in sample X21 at 50 °C, and that in b) reveals nearly complete solvation in sample X3 at 70 °C.

CONCLUSIONS

1. The developed solvent system of co-solvent MIM and ionic liquid EMIMAc is highly effective for cellulose and xylan solvation on a small scale. Both cellulose and xylan tend to aggregate in certain co-solvent/solvent mixtures where solubility is poor.
2. The solvation of cellulose in the solvent system is highly dependent on the EMIMAc-to-AGU ratio. When cellulose solubility is low in the system, solubility is further decreased as fiber length is increased. The effect is more pronounced at 50 °C than at 30 °C.
3. Slightly more than three acetate ions per AGU are required to solvate cellulose in the present system. This translates to an IL concentration of 6 to 8 mol % in MIM or 3 to 4 mol % IL per AGU.
4. Xylan solubility is greatly influenced by the temperature in the system. A temperature of 70 °C always gives a higher solubility compared to 50 °C. For experiments performed at 70 °C, a solubility plateau is reached at 3 mol % IL per AXU. A

concentration of 26 mol % of IL in MIM, equal to 9 mol % IL per AXU, most efficiently solvates the beech xylan at 50 °C.

5. FBRM probe technology can be used as an efficient tool for *in situ* monitoring of the solvation of both cellulose and xylan. The FBRM can detect variations in solubility with temperature in solvent mixtures of poor cellulose solubility that are difficult to detect with other methods.

ACKNOWLEDGMENTS

For the financial support of this work, which was conducted within the Wallenberg Wood Science Center, the authors would like to thank the Knut and Alice Wallenberg Foundation and Avancell (a collaboration between Chalmers University of Technology and Södra). Furthermore, Dr. Merima Hasani (Chalmers University of Technology) is gratefully acknowledged for professional advice and fruitful discussions.

REFERENCES CITED

Aaltonen, O., and Jauhiainen, O. (2009). "The preparation of lignocellulosic aerogels from ionic liquid solutions," *Carbohydrate Polymers* 75, 125-129.

Alfano, J. C., Carter, P. W., and Gerli, A. (1998). "Characterization of the flocculation dynamics in a papermaking system by non-imaging reflectance scanning laser microscopy (SLM)," *Nordic Pulp & Paper Research Journal* 13(2), 159-165.

Aspinall, G. O., Hirst, E. L., and Mahomed, R. S. (1954). "Hemicellulose A of beech-wood (*Fagus sylvatica*)," *Journal of the Chemical Society (Resumed)*, 1734-1738.

Bergenstråhle, M., Mazeau, K., and Berglund, L. A. (2008). "Molecular modeling of interfaces between cellulose crystals and surrounding molecules: Effects of caprolactone surface grafting," *European Polymer Journal* 44(11), 3662-3669.

Biermann, O., Hädicke, E., Koltzenburg, S., and Müller-Plathe, F. (2001). "Hydrophilicity and lipophilicity of cellulose crystal surfaces," *Angewandte Chemie International Edition* 40(20), 3822-3825.

Brodeur, G., Yau, E., Badal, K., Collier, J., Ramachandran, K. B., and Ramakrishnan, S. (2011). "Chemical and physicochemical pretreatment of lignocellulosic biomass: A review," *Enzyme Research*, Vol. 2011, article 787532, 17 pp.

Chen, M., Bomble, Y. J., Himmel, M. E., and Brady, J. W. (2012). "Molecular dynamics simulations of the interaction of glucose with imidazole in aqueous solution," *Carbohydrate Research* 349(0), 73-77.

Cho, H. M., Gross, A. S., and Chu, J.-W. (2011). "Dissecting force interactions in cellulose deconstruction reveals the required solvent versatility for overcoming biomass recalcitrance," *Journal of the American Chemical Society* 133(35), 14033-14041.

Coutant, C. A., Skibic, M. J., Doddridge, G. D., Kemp, C. A., and Sperry, D. C. (2010). "In vitro monitoring of dissolution of an immediate release tablet by focused beam reflectance measurement," *Molecular Pharmaceutics* 7(5), 1508-1515.

Cuissinat, C., Navard, P. N., and Heinze, T. (2008). "Swelling and dissolution of cellulose. Part IV: Free floating cotton and wood fibres in ionic liquids," *Carbohydrate Polymers* 72, 590-596.

Dence, C. W. (1992). "The determination of lignin," *Methods in Lignin Chemistry*, NC, 33-61.

Elnashaie, S. S. E. H., Fateen, S.-E., El-Ahwany, A., and Moustafa, T. M. (2008). "Integrated system approach to sustainability bio-fuels and bio-refineries," *Bulletin of Science, Technology & Society* 28(6), 510-520.

Fengel, D. W. (2011). *Wood: Chemistry, Ultrastructure, Reactions*, Walter de Gruyter, Berlin, DEU.

Fukaya, Y., Hayashi, K., Wada, M., and Ohno, H. (2008). "Cellulose dissolution with polar ionic liquids under mild conditions: Required factors for anions," *Green Chem.* 10, 44-46.

Gericke, M., Liebert, T., El, S. O. A., and Heinze, T. (2011). "Tailored media for homogeneous cellulose chemistry: Ionic liquid/co-solvent mixtures," *Macromol. Mater. Eng.* 296(6), 483-493.

Gericke, M., Schaller, J., Liebert, T., Fardim, P., Meister, F., and Heinze, T. (2012). "Studies on the tosylation of cellulose in mixtures of ionic liquids and a co-solvent," *Carbohydr. Polym.* 89(2), 526-536.

Gírio, F. M., Fonseca, C., Carvalheiro, F., Duarte, L. C., Marques, S., and Bogel-Łukasik, R. (2010). "Hemicelluloses for fuel ethanol: A review," *Bioresource Technology* 101(13), 4775-4800.

Gross, A. S., and Chu, J.-W. (2010). "On the molecular origins of biomass recalcitrance: The interaction network and solvation structures of cellulose microfibrils," *The Journal of Physical Chemistry B* 114(42), 13333-13341.

Gröndahl, M., Eriksson, L., and Gatenholm, P. (2004). "Material properties of plasticized hardwood xylans for potential application as oxygen barrier films," *Biomacromolecules* 5(4), 1528-1535.

Kosan, B., Michels, C., and Meister, F. (2008). "Dissolution and forming of cellulose with ionic liquids," *Cellulose* 15, 59-66.

Laus, G., Bentivoglio, G., Schottenberger, H., Kahlenberg, V., Kopacka, H., Röder, T., and Sixta, H. (2005). "Ionic liquids: Current developments, potential and drawbacks for industrial applications," *Lenzinger Berichte* 84, 71-85.

Lindman, B. (2010). "Amphiphilic biopolymers," *Colloids in Biotechnology*, M. Fanun (ed.), CRC Press, 1-7.

Lindman, B., Karlström, G., and Stigsson, L. (2010). "On the mechanism of dissolution of cellulose," *Journal of Molecular Liquids* 156(1), 76-81.

Linhardt, S. M. a. R. J. (2005). "Ionic liquids in carbohydrate chemistry – Current trends and future directions," *Current Organic Synthesis* 2, 437-451.

Liu, H., Cheng, G., Kent, M., Stavila, V., Simmons, B. A., Sale, K. L., and Singh, S. (2012a). "Simulations reveal conformational changes of methylhydroxyl groups during dissolution of cellulose Iβ in ionic liquid 1-ethyl-3-methylimidazolium acetate," *The Journal of Physical Chemistry B* 116(28), 8131-8138.

Liu, H., Sale, K. L., Holmes, B. M., Simmons, B. A., and Singh, S. (2010). "Understanding the interactions of cellulose with ionic liquids: A molecular dynamics study," *The Journal of Physical Chemistry B* 114(12), 4293-4301.

Liu, S., Lu, H., Hu, R., Shupe, A., Lin, L., and Liang, B. (2012b). "A sustainable woody biomass biorefinery," *Biotechnology Advances* 30(4), 785-810.

Liu, W., Wei, H., Zhao, J., Black, S., and Sun, C. (2013). "Investigation into the cooling crystallization and transformations of carbamazepine using in situ FBRM and PVM," *Organic Process Research & Development* 17(11), 1406-1412.

Liu, Z., Wang, H., Li, Z., Lu, X., Zhang, X., Zhang, S., and Zhou, K. (2011). "Characterization of the regenerated cellulose films in ionic liquids and rheological properties of the solutions," *Materials Chemistry and Physics* 128(1-2), 220-227.

Medronho, B., Romano, A., Miguel, M., Stigsson, L., and Lindman, B. (2012). "Rationalizing cellulose (in)solubility: Reviewing basic physicochemical aspects and role of hydrophobic interactions," *Cellulose* 19(3), 581-587.

Muhammad, N., Man, Z., Bustam, M., Mutalib, M. I. A., Wilfred, C., and Rafiq, S. (2011). "Dissolution and delignification of bamboo biomass using amino acid-based ionic liquid," *Applied Biochemistry and Biotechnology* 165(3-4), 998-1009.

O'Sullivan, A. (1997). "Cellulose: The structure slowly unravels," *Cellulose* 4(3), 173-207.

Rabideau, B. D., Agarwal, A., and Ismail, A. E. (2013). "Observed mechanism for the breakup of small bundles of cellulose Iα and Iβ in ionic liquids from molecular dynamics simulations," *The Journal of Physical Chemistry B* 117(13), 3469-3479.

Remsing, R. C., Petrik, I. D., Liu, Z., and Moyna, G. (2010). "Comment on 'NMR spectroscopic studies of cellobiose solvation in EmimAc aimed to understand the dissolution mechanism of cellulose in ionic liquids' by J. Zhang, H. Zhang, J. Wu, J. Zhang, J. He and J. Xiang, Phys. Chem. Chem. Phys., 2010, 12, 1941," *Physical Chemistry Chemical Physics* 12(44), 14827-14828.

Rettenmaier, N., Köppen, S., Gärtner, S. O., and Reinhardt, G. A. (2010). "Life cycle assessment of selected future energy crops for Europe," *Biofuels, Bioproducts and Biorefining* 4(6), 620-636.

Rinaldi, R. (2011). "Instantaneous dissolution of cellulose in organic electrolyte solutions," *Chemical Communications* 47(1), 511-513.

Rødsrud, G., Lersch, M., and Sjöde, A. (2012). "History and future of world's most advanced biorefinery in operation," *Biomass and Bioenergy* 46, 46-59.

Swatloski, R. P., Spear, S. K., Holbrey, J. D., and Rogers, R. D. (2002). "Dissolution of cellose with ionic liquids," *J. of the American Chemical Society* 124(18), 4974-4975.

Theander, O., and Westerlund, E. A. (1986). "Studies on dietary fiber. 3. Improved procedures for analysis of dietary fiber," *Journal of Agricultural and Food Chemistry* 34(2), 330-336.

Vanderhart, D. L., and Atalla, R. H. (1984). "Studies of microstructure in native celluloses using solid-state carbon-13 NMR," *Macromolecules* 17(8), 1465-1472.

Wendler, F., Todi, L.-N., and Meister, F. (2012). "Thermostability of imidazolium ionic liquids as direct solvents for cellulose," *Thermochimica Acta* 528, 76-84.

Wigell, A., Brelid, H., and Theliander, H. (2007). "Degradation/dissolution of softwood hemicellulose during alkaline cooking at different temperatures and alkali concentrations," *Nord. Pulp Pap. Res. J.* 22, 488-494.

Vitz, J., Erdmenger, T., Haensch, C., and Schubert, U. S. (2009). "Extended dissolution studies of cellulose in imidazolium based ionic liquids," *Green Chem.* 11(3), 417-424.

Youngs, T. G. A., Hardacre, C., and Holbrey, J. D. (2007). "Glucose solvation by the ionic liquid 1,3-dimethylimidazolium chloride: A simulation study," *The Journal of Physical Chemistry B* 111(49), 13765-13774.

Zakrajšek, N., Fuente, E., Blanco, A., and Golob, J. (2009). "Influence of cationic starch adsorption on fiber flocculation," *Chem. Eng. & Technology* 32(8), 1259-1265.

Article submitted: October 15, 2013; Peer review completed: December 16, 2013; Revised version accepted: December 19, 2013; Published: December 23, 2013.